Soft Matter

Accepted Manuscript

This article can be cited before page numbers have been issued, to do this please use: D. Berzi, M. M. Gianetti and D. Vescovi, *Soft Matter*, 2026, DOI: 10.1039/D6SM00233A.

ROYAL SOCIETY OF CHEMISTRY

rsc.li/soft-matter-journal

View Article Online
DOI: 10.1039/D6SM00233A

Superlubricity in granular shear flows under external vibrations

Diego Berzi*
Department of Civil and Environmental Engineering, Politecnico di Milano, 20133 Milano, Italy and Department of Mechanical Engineering, University of Victoria, Victoria, BC V8W 2Y2, Canada

Melisa M. Gianetti and Dalila Vescovi
Department of Civil and Environmental Engineering, Politecnico di Milano, 20133 Milano, Italy

(Dated: May 26, 2026)

We investigate the use of external vibrations to reduce macroscopic friction in pressure-imposed granular flows sheared between bumpy planes, in the absence of gravity, using the discrete element method. We observe that the system becomes superlubric, i.e., the macroscopic friction is less than 0.01, if one of the bumpy planes oscillates with a sufficiently large velocity amplitude. We quantify the reduction in the energy dissipated by the system through the work of the shear stress induced by the reduction in macroscopic friction and the external energy required to make the bumpy plane oscillate for different combinations of amplitude and frequency, and imposed pressure. We propose a phase-diagram and criteria in terms of imposed pressure and velocity amplitude of oscillations to predict the resistance to shear.

While lubrication properties of viscous fluids placed between solid surfaces are well known and extensively exploited in engineering applications, the possibility of using granular materials to reduce friction are relatively unexplored.

When particles are sheared between two parallel planes under an imposed normal load, they exert tangential forces on the planes. We call macroscopic friction, μ, the ratio of the tangential to the normal force. It is well known that macroscopic friction is nonzero even if the surface friction of the particles, associated with their microscopic asperities, is zero [1, 2]. The lubricant potential of granular materials crucially depends on identifying the parameters that control macroscopic friction. These parameters can be either internal–that is, the microscopic properties of the particles and the particle-particle interactions– or external –that is, external fields and boundary conditions.

Investigating the role played by the internal parameters is experimentally challenging. It is much easier to perform numerical simulations based on the Discrete Element Method (DEM) [3]. Previous works showed that reducing the coefficient of normal restitution (the negative of the ratio of the normal relative velocity after and before a collision between two spheres) also reduces the macroscopic friction, at least in the case of random assemblies of identical frictionless particles [4–6]. Indeed, it was shown that shearing flows of identical frictionless spheres crystallize if the pressure is larger than a minimum value, leading to a substantial increase in macroscopic friction [6]. Near this minimum value, using frictional rather than frictionless particles can reduce the macroscopic friction [7]. At larger pressures, which are more relevant for practical applications, the macroscopic friction is independent of the surface friction of the particles [7].

Manipulating the macroscopic friction through the geometry [8–10] or the motion of solid boundaries in contact with the granular materials is more appealing for practical purposes. DEM simulations have provided some evidence that the roughness of the boundaries has a significant effect on the overall flow resistance exerted on the granular flows, in the presence [11] and in the absence [6] of gravity. Some spectacular results of macroscopic friction reduction in granular materials stirred by a boundary have been observed in experiments [12, 13].

Intuitively, vibrating the boundary can also reduce macroscopic friction, at least when it induces fluidization in granular assemblies with a network of persisting contacts [14]. Friction reduction through vibrations is a process highly relevant to natural phenomena such as landslides and earthquakes [15–17]. The results of DEM simulations on poly-disperse, frictionless spheres sheared between two irregular planes under quasi-static conditions [18] indicate that frictional weakening requires (i) sufficient peak acceleration and (ii) a large ratio of the squared amplitude over the pressure to disrupt the contact network. Frictional weakening disappears when the vibration frequency exceeds the elastic response of the grains.

In this Letter, we perform DEM simulations of monodisperse, frictionless spheres sheared between two regular bumpy planes, in the absence of gravity, under imposed-pressure, while vibrating one of the boundaries. The aim is to investigate the frictional response of the system to the frequency and amplitude of vibrations, in the limit of sufficiently rigid spheres, for arbitrary values of the imposed pressure and the relative velocity between the planes. Thus, we generalize a previous work [18] that was limited to extremely high pressures and/or slow flows. We show that external vibrations allow us to achieve superlubricity [19, 20], a state of vanishing friction conventionally defined in engineering applications when $\mu < 0.01$ [21], at arbitrary values of the imposed

View Article Online
DOI: 10.1039/D6SM00233A

pressure and the relative velocity between the planes. In addition, we provide an energy analysis and find that, while friction can be dramatically reduced in the presence of vibrations, reaching superlubricity is an energy demanding endeavor.

We use the software LAMMPS [1] [22] for the DEM simulations. We randomly place $N = 3150$ identical spheres of diameter d and mass density ρ_p in a rectangular box of length $L_\mathrm{x} = 20d$, width $L_\mathrm{y} \approx 10d$, and initial height $L_\mathrm{z} \approx 20d$, with x, y, and z being the flow, vorticity, and gradient directions, respectively. The particles are confined between two rigid planes normal to the z-direction, constructed by gluing a layer of particles identical to the flowing particles in a hexagonal closed-packed arrangement. Each plane contains $N_\mathrm{w} = 240$ particles, and H is their relative distance. The shearing plane at $z = H$ experiences a constant pressure p and moves at constant velocity V along x, while being free to move along z as a rigid body. The vibrating plane at $z = 0$ oscillates harmonically as a rigid body along the z-axis with amplitude A and frequency f. Periodic boundary conditions are applied in the x- and y-directions. A snapshot of the simulations with the reference frame is shown in Figure 1.

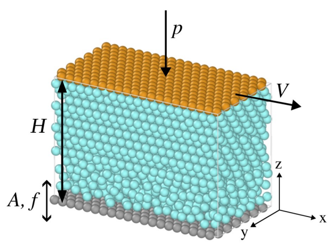

FIG. 1. Snapshot of the simulations, with the moving particles in cyan, the shearing plane in orange and the vibrating plane in gray. The number of moving particles in the simulations ($N = 3150$) is sufficiently large not to play a role [18].

Particle mass density ρ_p, diameter d, and velocity V of the shearing plane are the natural units of the system. Particles interact through the classic linear spring-dashpot contact model [3]. Unless stated otherwise, we set the microscopic sliding friction coefficient $\mu_p = 0$; the coefficient of normal restitution $e_n = 0.9$, as experimentally measured in collisions of glass beads [23]; and the normal spring stiffness $k_n = 10^4 pd$, or equivalently the Young modulus $E = k_n/d = 10^4 p$. As customary, the time step of the simulations is one fiftieth of the contact time [24]. The role of gravity is negligible as long as the difference in pressure between the shearing and the vibrating planes, Δp, is much smaller than p. Given that the extra-pressure is due to the weight of the N particles per unit basal area, the above criterion implies $p \gg N \rho_p g \pi d^3 / (6 L_x L_y) \approx 10 \rho_p g d$, where g is the gravitational acceleration.

We vary the imposed pressure $p/\left(\rho_p V^2\right)$ between 1 and 100, the frequency fd/V of the vibrating plane between 0 and 10, and the amplitude A/d between 0.1 and 2. Then, in our simulations, the parameter $A^2 E/\left(d^2 p\right)$ [18] is much larger than one, and the particle elastic modulus plays no role in controlling the frictional weakening effect of vibrations. This seems reasonable in many practical applications, where the Young modulus of sand grains or industrial metallic particles is of the order of 10^{10} Pa.

After an initial transient, the system reaches a steady state. Figure 2a shows the temporal evolution of height H/d once the steady state is attained, when $p/\left(\rho_p V^2\right) = 1$, $A/d = 1$, and $fd/V = 0$, 0.1, 0.2, and 1. At low frequency, fluctuations in H are small, and the system is in a dense state with a crystallized region near the sharing plane and a disordered region near the vibrating plane (Figure 2b). As the frequency increases, the region near the vibrating plane becomes more dilute. At a particular frequency, large fluctuations in H appear. Figure 2c shows the ratio of the time-averaged standard deviation of H, σ_H, over the time-averaged height, $\bar{H}$, as a function of $\Gamma = \rho_p d A \left(2\pi f\right)^2 / p$, the ratio of the peak acceleration induced by the vibrating boundary, $A\left(2\pi f\right)^2$, to the acceleration induced by the imposed pressure $p/\left(\rho_p d\right)$. As already pointed out [18, 25], $\Gamma = 1$ indicates when the vibration is strong enough to cause the detachment of the particles from the boundary. Also, in the quasi-static limit ($p/\left(\rho_p V^2\right) = 10^8$), $\Gamma > 1$ was necessary to observe the vanishing of macroscopic friction [18]. Figure 2c indicates that fluctuations in H begin to grow when $\Gamma = 0.1$, reach a peak around $\Gamma = 1.5$ and then abruptly decrease, in a manner that resembles the bouncing dynamics of an elastic body [26] (see Supplemental Material [27]). The slight increase of $\sigma_H/\bar{H}$ when Γ exceeds 10 is actually associated with bifurcation in the distribution of distances H/d (Supplemental Material [27]).

We measure macroscopic friction μ as the ratio between the tangential force, averaged over time, exerted by the flowing particles on the shearing plane per unit area of the plane and the imposed pressure. Notice that in the absence of gravity, the stresses in the steady state are homogeneous in the domain. If vibrations are the dominant mechanism, we expect that the shear stress exerted by the particles on the shearing plane is given by their momentum in the x-direction, $\rho_p d V$, times its rate of exchange, with the latter set by the angular frequency, $2\pi f$, of the vibrating plane. Similarly, the normal stress (pressure) should be proportional to the momentum in the z-direction, $\rho_p d 2\pi f A$ ($2\pi f A$ is the typical velocity in the z-direction), times the exchange rate, $2\pi f$. Then, at large frequencies, we expect μ to be inversely proportional to the dimensionless velocity amplitude $2\pi f A/V$, independent of the pressure.

We already know that, in the absence of vibrations,

[1] www.lammps.org

View Article Online
DOI: 10.1039/D6SM00233A

$\mu = \mu_0$ is only a function of $p/\left(\rho_p V^2\right)$. The dependence of μ_0 on the imposed pressure is shown in the Supplemental Material [27] and agrees very well with the measurements on frictionless poly-disperse spheres sheared between planes of irregular geometry [18], thus suggesting that our findings are not limited to crystallized systems. Given that $\mu_0 = \mu_0\left(p/\left(\rho_p V^2\right)\right)$, there must be a range of velocity amplitudes, between 0 and a characteristic value, in which the macroscopic friction is influenced by the imposed pressure, followed by a collapse onto a universal, pressure-independent curve. The measurements reported in Figure 3a confirm the collapse and permit fitting the expression of the universal curve as $\mu \approx 0.1\left(2\pi f A/V\right)^{-1}$. The error bars estimated on bootstrap resampling [28] are smaller than the symbols in Figure 3a and in the remainder of the figures. From the latter, we can calculate the velocity amplitude at which the pressure-independent macroscopic friction reaches the superlubricity limit as $2\pi f A/V = 10$. The characteristic velocity amplitude marking the collapse onto the pressure-independent curve is, in itself, pressure-dependent. As shown later, a simple experimental criterion based on Γ allows us to identify it.

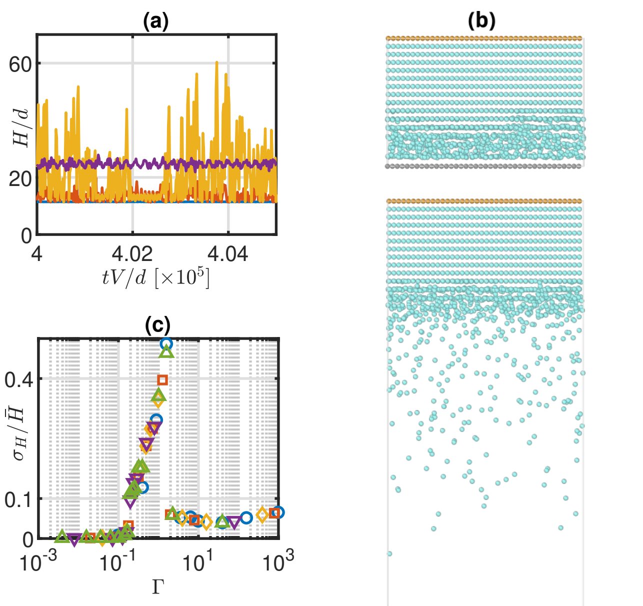

FIG. 2. (a) Temporal evolution of H/d when $p/\left(\rho_p V^2\right) = 1$, $A/d = 1$, and: $fd/V = 0$ (blue line); $fd/V = 0.1$ (orange line); $fd/V = 0.2$ (yellow line); and $fd/V = 1$ (purple line). (b) Snapshots of the simulation at two times, corresponding to small and large distance between the planes, when $p/\left(\rho_p V^2\right) = 1$, $A/d = 1$, and $fd/V = 0.2$. (c) Ratio of the time-averaged standard deviation of H, σ_H, over the time-averaged height, $\bar{H}$, as a function of Γ for all data with $A/d = 1$ (different colors and symbols correspond to different pressures, as detailed in the caption of Figure 3.).

Vibrations, therefore, permit to reach superlubricity, which is certainly desirable to drastically reduce wear and the energy dissipated through shearing. However, energy must be injected into the system to provide vibrations.

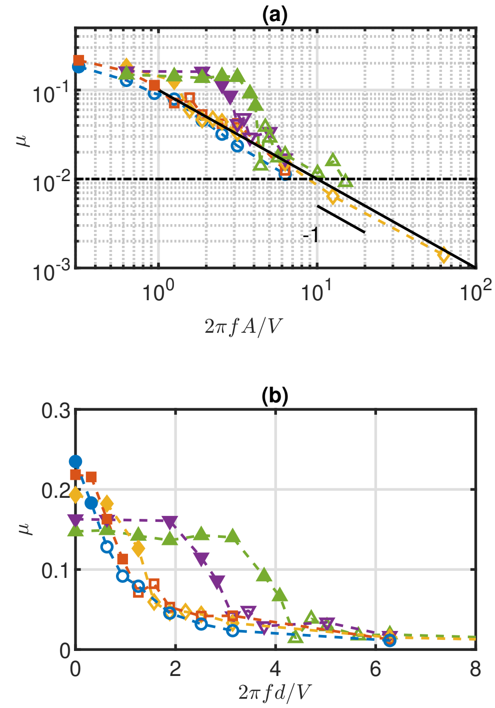

FIG. 3. (a) Macroscopic friction as a function of the velocity amplitude measured in the simulations for various A/d and: $p/\left(\rho_p V^2\right) = 1$ (blue circles); $p/\left(\rho_p V^2\right) = 5$ (orange squares); $p/\left(\rho_p V^2\right) = 10$ (yellow diamonds); $p/\left(\rho_p V^2\right) = 50$ (purple lower triangles); $p/\left(\rho_p V^2\right) = 100$ (green upper triangles). Also shown are the superlubricity limit (black dot-dashed line) and the pressure-independent limit $\mu = 0.1\left(2\pi f A/V\right)^{-1}$ (black solid line). (b) Measured macroscopic friction as a function of $2\pi f d/V$ when $A/d = 1$ (linear scale). Filled and open symbols (connected by dashed lines to guide the eyes) represent measurements relative to the pressure-dependent and pressure-independent regime for the macroscopic friction, respectively.

The dissipated power per unit area of the shearing plane in the absence of vibrations due to the work of the tangential force is given by $\mu_0 p V$, where μ_0 is the macroscopic friction when $2\pi f A = 0$. The corresponding dissipated power per unit area of the shearing plane in the presence of vibrations is $\mu p V$. The power per unit area required to vibrate the plane can be calculated as the sum of: (i) the mean kinetic energy of the plane over one period, $M\left(2\pi f A\right)^2/4$, with M the mass of the plane, divided by the period, $1/f$, the area of the plane, $L_x L_y$, and a generic mechanical efficiency η; (ii) the work done to push against the granular materials over one half cycle of the sinusoidal motion of the plane, $p\left(2/\pi\right)2\pi f A$, since the plane moves away from the dry assembly of cohesionless particles at no cost.

View Article Online
DOI: 10.1039/D6SM00233A

We define the energy penalty as

$$\begin{aligned}\varepsilon &= \frac{1}{\mu_0 pV}\left[\mu pV + \frac{M\left(2\pi f A\right)^2 f}{4L_xL_y\eta} + p\frac{2}{\pi}2\pi f A - \mu_0 pV\right] \\ &= \frac{\mu}{\mu_0} + \frac{1}{\mu_0}\frac{1}{24\eta\sqrt{3}}\left(\frac{2\pi f d}{V}\right)^3\frac{\rho_p V^2}{p}\left(\frac{A}{d}\right)^2 \\ &\quad + \frac{2}{\mu_0\pi}\frac{2\pi f d}{V}\frac{A}{d} - 1, \qquad (1)\end{aligned}$$

where we have used the fact that in our case $M = N_w\rho_p\pi d^3/6$ and $L_xL_y = N_w\pi d^2/\left(4\phi_{HCP}\right)$, with $\phi_{HCP} = \pi/\left(2\sqrt{3}\right)$ being the area fraction of a hexagonal close packing of disks. At the superlubricity limit $2\pi f A/V = 10$, the work done to push against the granular material is the dominant contribution to the energy penalty if $p/\left(\rho_p V^2\right) \gg 5$. Then, with $\mu_0 \approx 0.2$, reaching superlubricity, that is, a twenty-fold decrease in the macroscopic friction, requires a $(2/\pi)\,10/0.2 \approx 50$-fold increase in the energy input.

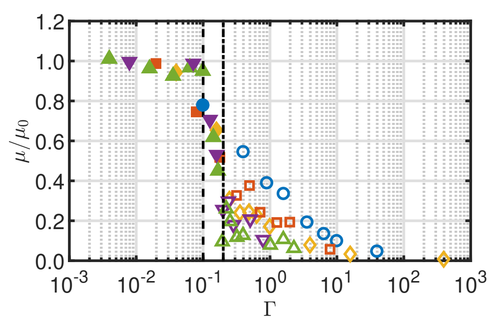

FIG. 4. Macroscopic friction normalized by its value in the absence of vibrations as a function of Γ for all data with $A/d = 1$. Same legend as in Figure 3. Also shown are the minimum value of $\Gamma = 0.1$ (dashed line) for observing the influence of the velocity amplitude and the value $\Gamma = 0.2$ (dot-dashed line) above which the macroscopic friction is pressure-independent.

Figure 4 shows that the vibrations begin to reduce the macroscopic friction when Γ is about 0.1, that is the same value at which the fluctuations in the gap between the planes start to grow (Figure 2c). Given the definition of Γ, $\Gamma = 0.1$ corresponds to

$$\frac{2\pi f A}{V} = \left(\frac{1}{10}\right)^{1/2}\left(\frac{A}{d}\right)^{1/2}\left(\frac{p}{\rho_p V^2}\right)^{1/2}, \qquad (2)$$

which gives the minimum velocity amplitude to observe frictional weakening.

Figure 4 also suggests that macroscopic friction enters the pressure-independent regime (open symbols) once the parameter Γ is greater than 0.2, that is, when the velocity amplitude is greater than

$$\frac{2\pi f A}{V} = \left(\frac{1}{5}\right)^{1/2}\left(\frac{A}{d}\right)^{1/2}\left(\frac{p}{\rho_p V^2}\right)^{1/2}. \qquad (3)$$

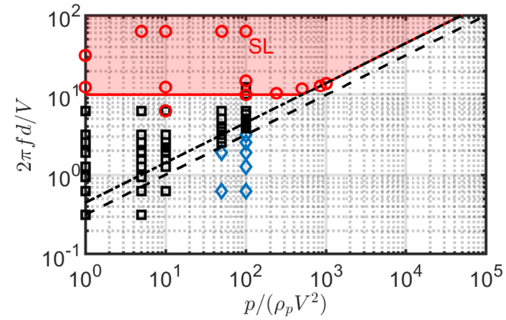

FIG. 5. Phase-diagram for pressure-imposed shearing flows in the presence of vibrations, when $A/d = 1$ and: no frictional weakening is observed (blue diamonds); frictional weakening is present but $\mu > 0.01$ (black squares); the flow is superlubric (red circles). The red area represents the region in the phase-diagram where we expect superlubricity. Dashed and dot-dashed line correspond to equations (2) and (3), respectively.

We can now build a phase-diagram to characterize the behavior of pressure-imposed shearing flows subjected to external vibrations, in the limit of rigid particles, and, for simplicity, when $A/d = 1$. Then, the only control parameters are $p/\left(\rho_p V^2\right)$ and $2\pi f d/V$.

First, frictional weakening induced by vibrations is observed if the velocity amplitude is greater than the value given by equation (2) (the region above the dashed line in Figure 5). Second, in the region above the dot-dashed line in Figure (5), the macroscopic friction does not depend on the pressure but only on the velocity amplitude. Finally, superlubricity is achieved whenever the velocity amplitude is greater than the value given by equation (3), i.e., the macroscopic friction enters its pressure-independent regime, provided that it is also greater than 10 (red area in Figure 5).

Here, we have focused on frictionless spheres interacting through linear contact. If we employ frictional particles, the dependence of the macroscopic friction and the efficiency gain on the velocity amplitude is qualitatively similar. As expected, the macroscopic friction for frictional particles is slightly larger than in the frictionless case (see Supplemental Material [27]). Our results, and in particular the phase-diagram for the search for low-wearing operational conditions of vibrated shearing flows of granular materials, are therefore robust and only mildly affected by the frictional properties of the particles, their size distribution, the geometry of the shearing planes, and the contact law [18].

AUTHOR CONTRIBUTIONS

DB: Conceptualization, Formal analysis, Writing – Original Draft, Methodology, Visualization. MMG: Investigation, Data Curation, Software, Writing – review

View Article Online
DOI: 10.1039/D6SM00233A

& editing. DV: Conceptualization, Software, Writing – review & editing, Supervision.

DATA AVAILABILITY

Data for this article are available at Zenodo at: https://doi.org/10.5281/zenodo.20343433.

CONFLICTS OF INTEREST

There are no conflicts to declare.

ACKNOWLEDGEMENTS

This project has received funding from the HORIZON-EIC-2021- PATHFINDEROPEN-01 N. 101046693, SSLiP project. Funded by the European Union. Views and opinions expressed are however those of the author(s) only and do not necessarily reflect those of the European Union or EIC. Neither the European Union nor the granting authority can be held responsible for them.

* diego.berzi@polimi.it

[1] P.-E. Peyneau, J.-N. Roux, A. Co, G. L. Leal, R. H. Colby, and a. Jeffrey Giacomin, Shear flow of sphere packings in the geometric limit, AIP Conf. Proc. **1027**, 947 (2008).
[2] D. Vescovi and S. Luding, Merging fluid and solid granular behavior, Soft Matter **12**, 8616 (2016).
[3] P. A. Cundall and O. D. L. Strack, A discrete numerical model for granular assemblies, Geotechnique **29**, 47 (1979).
[4] D. Vescovi, D. Berzi, P. Richard, and N. Brodu, Plane shear flows of frictionless spheres: Kinetic theory and 3d soft-sphere discrete element method simulations, Phys. Fluids **26**, 053305 (2014).
[5] D. Berzi and D. Vescovi, Shearing flows of frictionless spheres over bumpy planes: slip velocity, Computat. Part. Mech. **4**, 373 (2017).
[6] D. Vescovi, A. S. de Wijn, G. L. Cross, and D. Berzi, Extended kinetic theory applied to pressure-controlled shear flows of frictionless spheres between rigid, bumpy planes, Soft Matter **20**, 8702 (2024).
[7] E. Kurban, D. Vescovi, and D. Berzi, Crystallization in load-controlled shearing flows of monosized spheres, Soft Matter **21**, 2049 (2025).
[8] M. W. Richman, Boundary conditions based upon a modified maxwellian velocity distribution for flows of identical, smooth, nearly elastic spheres, Acta Mech. **75**, 227 (1988).
[9] J. T. Jenkins, Boundary conditions for rapid granular flow: Flat, frictional walls, Journal of Applied Mechanics **59**, 120 (1992).
[10] M. Louge and S. C. Keast, On dense granular flows down flat frictional inclines, Phys. Fluids **13**, 1213 (2001).
[11] V. Kumaran and S. Bharathraj, The effect of base roughness on the development of a dense granular flow down an inclined plane, Phys. Fluids **25**, 070604 (2013).
[12] K. Nichol, A. Zanin, R. Bastien, E. Wandersman, and M. V. Hecke, Flow-induced agitations create a granular fluid, Phys. Rev. Lett. **104**, 10.1103/PhysRevLett.104.078302 (2010).
[13] K. Nichol and M. V. Hecke, Flow-induced agitations create a granular fluid: Effective viscosity and fluctuations, Phys. Rev. E **85**, 10.1103/PhysRevE.85.061309 (2012).
[14] M. G. Irmer, E. E. Brodsky, and A. H. Clark, Granular temperature controls local rheology of vibrated granular flows, Phys. Rev. Lett. **134**, 10.1103/PhysRevLett.134.048202 (2025).
[15] J. Léopoldès, X. Jia, A. Tourin, and A. Mangeney, Triggering granular avalanches with ultrasound, Phys. Rev. E **102**, 042901 (2020).
[16] V. Durand, A. Mangeney, P. Bernard, X. Jia, F. Bonilla, C. Satriano, J.-M. Saurel, E. M. Aissaoui, A. Peltier, V. Ferrazzini, P. Kowalski, F. Lauret, C. Brunet, and C. Hibert, Repetitive small seismicity coupled with rainfall can trigger large slope instabilities on metastable volcanic edifices, Commun. Earth Environ. **4** (2023).
[17] H. Martin, A. Mangeney, X. Jia, B. Maury, A. Lefebvre-Lepot, Y. Maday, and P. Dérand, Ultrasound-induced dense granular flows: a two-time scale modelling, J. Fluid Mech. **1004**, A10 (2025).
[18] A. H. Clark, E. E. Brodsky, H. J. Nasrin, and S. E. Taylor, Frictional weakening of vibrated granular flows, Phys. Rev. Lett. **130**, 118201 (2023).
[19] A. S. de Wijn, (in)commensurability, scaling, and multiplicity of friction in nanocrystals and application to gold nanocrystals on graphite, Phys. Rev. B **86**, 10.1103/physrevb.86.085429 (2012).
[20] J. A. van den Ende, A. S. de Wijn, and A. Fasolino, The effect of temperature and velocity on superlubricity, J. Phys.-Condens. Mat. **24**, 445009 (2012).
[21] X. Ge, Z. Chai, Q. Shi, Y. Liu, and W. Wang, Graphene superlubricity: A review (2023).
[22] A. P. Thompson, H. M. Aktulga, R. Berger, D. S. Bolintineanu, W. M. Brown, P. S. Crozier, P. J. in 't Veld, A. Kohlmeyer, S. G. Moore, T. D. Nguyen, R. Shan, M. J. Stevens, J. Tranchida, C. Trott, and S. J. Plimpton, Lammps - a flexible simulation tool for particle-based materials modeling at the atomic, meso, and continuum scales, Comput. Phys. Commun. **271**, 108171 (2022).
[23] S. F. Foerster, M. Y. Louge, H. Chang, and K. Allia, Measurements of the collision properties of small spheres, Phys. Fluids **6**, 1108 (1994).
[24] P. A. Thompson and G. S. Grest, Granular flow: Friction and the dilatancy transition, Phys. Rev. Lett. **67**, 1751 (1991).
[25] J. A. Dijksman, G. H. Wortel, L. T. V. Dellen, O. Dauchot, and M. V. Hecke, Jamming, yielding, and rheology of weakly vibrated granular media, Phys. Rev. Lett. **107**, 10.1103/PhysRevLett.107.108303 (2011).
[26] M. Hubert, F. Ludewig, S. Dorbolo, and N. Vandewalle, Bouncing dynamics of a spring, Physica D **272**, 1 (2014).
[27] See supplemental material at ... for additional text and figures supporting claims made in the main text on the fluctuations in the distance between the planes, the influence of poly-dispersity and geometry of the planes, the

View Article Online
DOI: 10.1039/D6SM00233A

dependence of the efficiency gain on the vibration amplitude, and the influence of sliding friction.
[28] B. Efron, *The Jackknife, the Bootstrap and Other Resampling Plans* (Society for Industrial and Applied Mathematics, Philadelphia, 1982).

View Article Online
DOI: 10.1039/D6SM00233A

Data for this article are available at Zenodo at:

https://doi.org/10.5281/zenodo.20343433